Physica Medica 102 (2022) 9–18

Contents lists available at ScienceDirect

Physica Medica

journal homepage: www.elsevier.com/locate/ejmp

A new solution for UHDP and UHDR (Flash) measurements: Theory and conceptual design of ALLS chamber

Fabio Di Martino [a,b,d,*], Damiano Del Sarto [b], Maria Giuseppina Bisogni [b,c,d], Simone Capaccioli [b,c], Federica Galante [e], Alessia Gasperini [f,g], Stefania Linsalata [a], Giulia Mariani [e], Matteo Pacitti [e], Fabiola Paiar [b,d,h], Stefano Ursino [b,d,h], Verdi Vanreusel [f,g], Dirk Verellen [f,g], Giuseppe Felici [e]

[a] Fisica Sanitaria, Azienda Ospedaliero Universitaria Pisa AOUP, ed.18 via Roma 67, Pisa, Italy
[b] Centro Pisano ricerca e implementazione clinica Flash Radiotherapy (CPFR@CISUP), Presidio S. Chiara, ed. 18 via Roma 67, Pisa, Italy
[c] Department of Physics, University of Pisa, Largo B. Pontecorvo 3, I-57127 Pisa, Italy
[d] INFN, Sezione di Pisa, Largo B. Pontecorvo 3, I-57127 Pisa, Italy
[e] SIT S.p.A., via del Commercio 1A, Aprilia (LT), Italy
[f] Iridium Kankernetwerk, 2610 Antwerp, Belgium
[g] Antwerp University, Faculty of Medicine and Health Sciences, 2610 Antwerp, Belgium
[h] Radiation Oncology Unit, Department of Translational Research, University of Pisa, Pisa, Italy

ARTICLE INFO

Keywords:
UHDP
FLASH
Gas chamber

ABSTRACT

Ultra-High dose-*per*-pulse regimens (UHDP), necessary to trigger the "FLASH" effect, still pose serious challenges to dosimetry. Dosimetry plays a crucial role, both to significantly improve the accuracy of the radiobiological experiments necessary to fully understand the mechanisms underlying the effect and its dependencies on the beam parameters, and to be able to translate such effect into clinical practice. The standard ionization chamber in UHDP region is significantly affected by the effects of the electric field generated by the enormous density of charges produced by the dose pulse.

This work describes the theory and the conceptual design of a gas chamber (the ***ALLS chamber***) which overcomes the above-mentioned problems.

Introduction

The FLASH effect [1,2] is a radiobiological effect obtained by delivering the entire therapeutic dose in less than 100 ms, thus allowing to drastically reduce the side effects for healthy tissues, still maintaining the same therapeutic efficacy on the tumor. This leads to a broadening of the therapeutic window.

The effect has been experimentally proved by different centres and on different animal models, arising great expectations in the scientific world because of its enormous clinical potential [3,4]. However, the full clinical implementation of the FLASH effect raises a series of technological, dosimetric and radiobiological issues to be addressed and solved. Radiation beams with dose-*per*-pulse and dose rate at least 2–3 orders of magnitude higher than those used in conventional radiotherapy are mandatory to trigger the FLASH effect. The radiobiological mechanisms underlying the effect and its quantitative dependencies on beam parameters and irradiated tissue are still not fully known [5–8].

Until early 2021, "active" dosimeters were not available to measure such beams properly [6–12]. Then, two promising new devices were presented and tested: the ultra-thin ionization chamber, mainly studied and developed by F. Gomez Rodriguez et al. [10–14], and the Flash diamond, developed by M. Marinelli and G. Verona Rinati et al. [15,16].

In this work a new theoretical approach to Ultra High Dose per Pulse (UHDP) and Ultra High Dose Rate (UHDR) measurements by means of a gas chamber is considered and discussed. In general, the analytical description of ion collection under such conditions is not feasible [13,14,17]. However, the general equation can be simplified by choosing some parameters properly so that an analytical description can be derived even in UHDP/UHDR conditions. Thanks to the above-mentioned tools, a new gas chamber model, called ALLS, has been

Abbreviations: UHDP, Ultra High Dose per Pulse.

* Corresponding author at: Fisica Sanitaria, Azienda Ospedaliero Universitaria Pisa AOUP, ed.18 via Roma 67, Pisa, Italy.
E-mail address: f.dimartino@ao-pisa.toscana.it (F. Di Martino).

https://doi.org/10.1016/j.ejmp.2022.08.010
Received 28 February 2022; Received in revised form 27 July 2022; Accepted 10 August 2022
Available online 27 August 2022

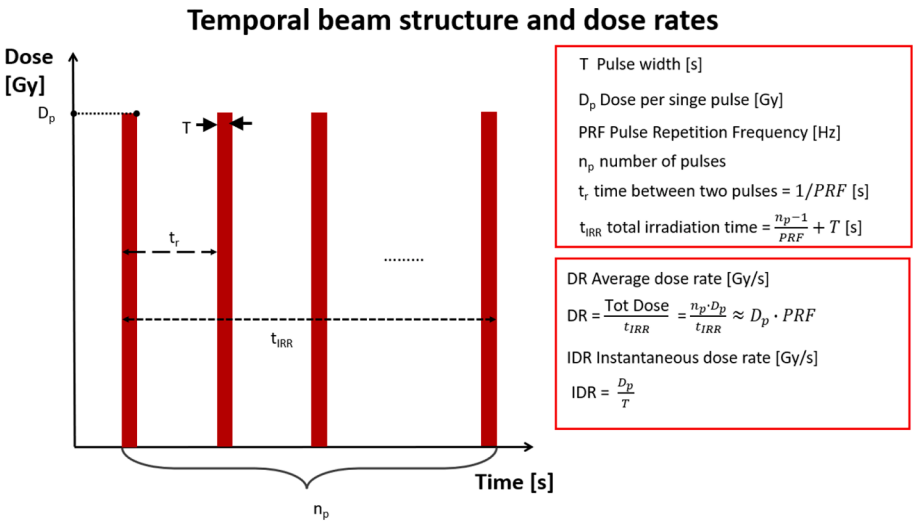

Fig. 1. Temporal beam structure and dose rate definition.

developed. Before describing the theory details, it is mandatory to identify some features of the UHDP/UHDR beams.

The minimal requirements a pulsed beam should meet for triggering the FLASH effect may be summarized as follows [18–21]:

- Total irradiation time below 100 ms;
- Dose per pulse above 1 Gy;
- Average dose rate above 40 Gy/s, probably above 100 Gy/s;
- Instantaneous dose rate above $2.5 \cdot 10^5$ Gy/s corresponding for example to a dose per pulse of 1 Gy delivered in a 4 μs pulse [20].

Since today there is no consensus on which beam parameters trigger precisely and optimize the 'FLASH' effect, the 'optimal dosimeter' should be capable of measuring any reasonable 'FLASH' dose per pulse and any dose rat. This work is focused on the theory that allows the design of ALLS chamber. The study herein presented assumes 40 Gy as the maximum dose per pulse, which would correspond to a single 40 Gy treatment delivered in a single pulse.

The standard ionization chambers and the main devices in the commissioning of medical accelerators, are unusable [11,13,19]. The classical formula to calculate the dose with an ionization chamber is (Eq. (1)) [22]:

$$D_w = N_{D,W,Q_0} M_Q k_{Q,Q_0} \quad (1)$$

Where Dw is dose measured in water, N_{D,W,Q_0} is the calibration factor of the chamber for a reference beam of quality Q_0, M_Q is the reading of the chamber (to be corrected for $k_{P,T}$, k_{sat}, k_{pol}, k_{elec}), k_{Q,Q_0} is the factor that corrects for the different quality of beam depending on calibration conditions. This approach is not applicable at UHDP values, because of the magnitude of the electric field generated by the ionized charges.

In the 'classical' case, the electric field is assumed to be generated by the external polarization voltage and to be constant across the chamber sensitive volume; such hypotheses are no longer valid in UHDP region. The electric field generated by the ionized charges can be intense enough both to nullify the overall field and to reach values (around 1000 V/mm in air) such that secondary generations can happen in different points inside the collecting volume.

Both these conditions cause the chamber to exit from the ionization regimen [19,11,14].

This work describes the theory and the conceptual design of the gas chamber *ALLS* [23] for the absolute on-line dosimetry of electron beams in FLASH regimen. This feature allows to overcome the above-mentioned problems with at least 1 % accuracy for dose-*per*-pulse values up to 40 Gy.

The ALLS chamber is mainly based on these complementary pillars: the use of a noble gas and the possibility of varying its pressure inside the chamber.

The choice of a noble gas allows to:

1. eliminate recombination issues (within 0.1 % [14], provided that the electric field is always and everywhere greater than zero;
2. allow the analytical description of the electric field during the charges collection process.

The adoption of a noble gas prevents the electron capture by gas molecules (as it happens with oxygen for air filled chambers [24]. Therefore, there is no generation of negative ions and the only possible recombination scenario remains the direct recombination between positive ions and electrons. Such recombination can be considered negligible if the electric field is always and everywhere greater than zero (within 0.1 % [14]). Electrons have a mobility at least three orders of magnitude higher than positive ions [25]. The difference in the mobility allows to divide the collection process into two different phases: positive ions are still considered during the electrons collection, then, only the positive charges are considered, since electrons are collected immediately (respect to ion dynamics) after being generated.

Such assumptions allow to describe the behaviour of the electric field analytically as a function of five parameters: the absorbed dose-*per*-pulse (related to the charge generated into the chamber in a pulse of radiation) D_p, the applied voltage V, the distance between the electrodes d, the density of the gas ρ and the pulse duration T.

Then, for any value of D_p of clinical utility, it is possible to vary the ALLS chamber parameters appropriately, in a way that:

1. the recombination is negligible (within 0.1 % [14]);
2. during the charge collection time, the electric field across the chamber will not lead to significant/uncontrolled charge multiplication;
3. the maximum perturbation of the electric field generated by the charges produced is such that the resulting inaccuracy (i.e the deviation from a linear charge-to-dose response) is less than a fixed threshold (in the following 1 % value is used) in the whole range of dose-*per*-pulse considered.

In this paper, the gas chamber theory is described step by step.

In order to provide a reasonable numerical example, whose values have been used to design the ALLS chamber prototype, the model refers to a plane parallel gas chamber filled with Argon, with distance between

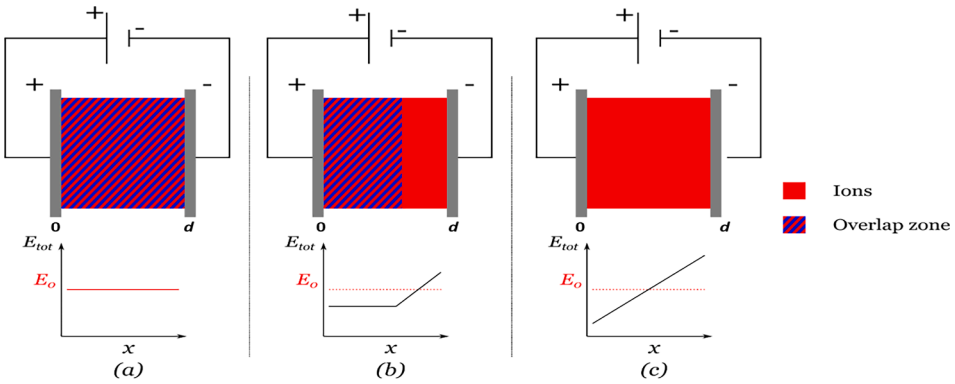

Fig. 2. (a) $t = 0$: at the beginning of the pulse there is an overlap between positive ions and electrons, the total field is E_0. (b) $0 < t <$ electron collection time: due to their higher mobility, electrons start to be collected near the positive electrode forming a net positive spatial charge near the cathode; this generates E_{ION} that is superimposed to E_0(c t) = T after complete electron collection the effect of E_{ION} is maximum, this is the limit condition considered to avoid recombination.

electrodes $d = 1$ mm, polarization bias $V = 200$ V.

Theory (materials and methods)

As explained above, a noble gas such as the chamber filler is considered and, in particular, for the ALLS chamber Argon is used. After a ionization process, the electrons generated migrate to the positive electrode without being captured and, since their mobility is at least three orders of magnitude higher than positive ions, no recombination happens when electric field is always and everywhere greater than zero.

It is convenient to define all the relevant beam parameters starting from the definitions of dose per pulse D_p and pulse duration T. Assuming that beam emission is nearly constant during T, instantaneous dose rate (IDR) or dose rate within the pulse $\dot{D}_p = \frac{D_p}{T}$ (see Fig. 1) are defined; average dose rate $DR = PRF \cdot D_p$ where PRF is the Pulse Repetition Frequency. It was chosen to start from the definition of dose per pulse and pulse duration (instead of introducing the dose rate directly) because these two parameters can be measured precisely and independently from each other.

The chamber behaviour analysis can be restricted to dynamics collection within a single pulse neglecting any residual charge from the previous pulse, because complete intra-pulse charge collection is achieved (see Appendix A) between one pulse and the next one.

The theory presented in this work describes the behavior of the ALLS chamber considering the absence of overlap between consecutive radiation pulses. This theoretical model is structured into three subsections, namely: ion/electron recombination, discharge regimen avoidance and evaluation of the maximum electric field perturbation within the chamber.

The ions/electrons recombination – How to avoid it

After a ionization event ($t = 0$), the electrons will move under the influence of the static field applied to the chamber, $\boldsymbol{E_0}$ (see Fig. 2, a); then, electron/positive ions overlap zone with zero net charge will be present in the chamber volume (see Fig. 2, b). Afterwards, electrons start to be collected near the anode while positive ions accumulate due to the mobility difference. As a result, a positive charge density will be generated near the anode (see Fig. 2, c). This positive charge distribution creates a perturbative field called $\boldsymbol{E_{ION}}(x,t)$, which will be added to $\boldsymbol{E_0}$. The total electric field $\boldsymbol{E}(x,t) = \boldsymbol{E_0}(x,t) + \boldsymbol{E_{ION}}(x,t)$ has a module that is monotonically increasing going from the positive (x = 0) to the negative (x = d) electrode (see Fig. 2); given the boundary conditions, $\boldsymbol{E_{ION}}$ and, as a consequence, $\boldsymbol{E}$, are one dimensional bi-directional vectors.

Therefore, considering electrons recombination, the most critical situation is represented when $\boldsymbol{E(x,t)}$ is minimum, that is at x = 0 and $t = T$, when all ions have been generated and, as additional conservative hypothesis, none of them has been already collected. (Fig. 2).

In the following, a plane parallel chamber is considered, with the two planar electrodes having an interelectrode distance $d \ll \sqrt{S}$, being S the electrode surface area.

Such hypothesis allows to neglect electric field boundary modification, to assume a cylindrical symmetry and, therefore, to adopt a one-dimensional approach to calculate the bulk electric field.

It is important to consider that the assumption of a noble gas and of the electrodes geometry dramatically simplifies the process modelling; it is now possible to obtain equations which can be solved analytically.

At $t = T$, an expression for the positive ions field $\boldsymbol{E_{ION}}(x,T)$ (Equation (3)) can be obtained by solving the Poisson equation (Equation (2)) in the reference frame with the x axis pointing toward the negative electrode of the chamber:

$$\frac{d^2 V}{dx^2} = -\frac{q_V^{gen}}{\varepsilon_0 \bullet \varepsilon_r} \tag{2}$$

where q_V^{gen} is the volumetric charge density ($Qv^{gen} = Q^{gen}/Vol$, where Q^{gen} is the charge generated) and ε_0, ε_r are the vacuum and the relative gas permittivity, respectively.

Then, with the above-mentioned assumptions, if the electric field is everywhere greater than zero at $t = T$, it can be inferred it is greater than zero also for any other time t.

Since for x = d/2 the positive ions electric field (E= − dV/dx) must be equal to 0 for symmetry Eq. (2) can be immediately integrated:

$$\boldsymbol{E_{ION}}(x,t) = \frac{q_V^{gen}}{\varepsilon_0 \varepsilon_r}\left(x - \frac{d}{2}\right)\hat{x} \tag{3}$$

Due to superposition principle, the total field (static and uniform chamber field plus ions perturbation field) is given by:

$$\boldsymbol{E} = \boldsymbol{E_0} + \boldsymbol{E_{ION}} \tag{4}$$

Based on our description in 1D it is possible to drop the vectorial formalism.

A precise constrain on the value of $\boldsymbol{E_0}$ is given by imposing:

$$\boldsymbol{E_0} + \boldsymbol{E_{ION}}(0) > 0 \tag{5}$$

that is:

$$\boldsymbol{E_0} > \frac{q_V^{gen}}{\epsilon_0 \epsilon_r}\frac{d}{2} \tag{6}$$

as long as, the chamber operates at fixed potential V and the integral of $\boldsymbol{E_{ION}}$ field gives a zero contribution, it is:

$$\int_0^d E\,dx = \int_0^d E_0\,dx + \int_0^d E_{ION}\,dx = V \Rightarrow E_0 = \frac{V}{d} \tag{7}$$

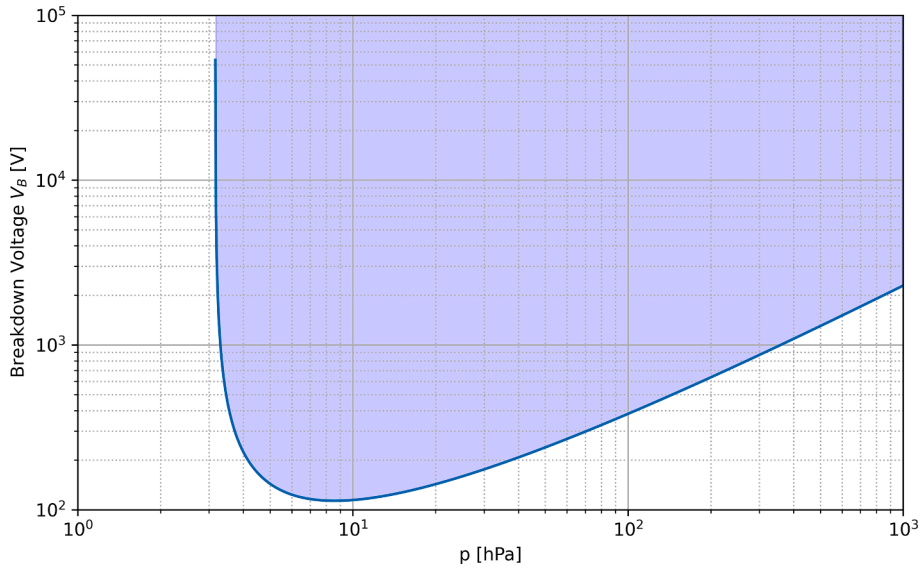

Fig. 3. Paschen curve for Argon at 1 mm electrodes distance; the blue area indicates the discharge region. (For interpretation of the references to colour in this figure legend, the reader is referred to the web version of this article.)

Table 1
ALLS operating parameters.

	Parameters	Value
Beam	*Pulse duration T*	4 μs
	Dose per pulse D_p	40 Gy
ALLS Chamber	*Electrodes distance d*	1 mm
	Argon Density ρ_0 *@ NTP*	1.66 kg m^{-3}
	Pressure	1 hPa
	Voltage	200 V
	Argon average energy w_e	26 eV
	Argon mobility μ_0 *@ NTP*	$1.6 \cdot 10^{-4}$ m^2 V^{-1} s^{-1}
	Argon dielectric constant $\varepsilon_0\varepsilon_r$	$8.85 \cdot 10^{-12}$ C V^{-1} m^{-1}

Table 2
Estimated relative uncertainty of the model parameters.

Quantity	Relative uncertainty
Electrodes distance d	0.1 %
Pressure P	1 %
Voltage V	0.01 %
Argon mobility μ_0 *@ NTP*	1 %
Argon average energy w_e	1 %
Chamber perturbation value $\left\|\frac{\Delta E}{E_0}\right\|$	4%

Fig. 4. ALLS chamber - conceptual drawing (left) and first prototype (right).

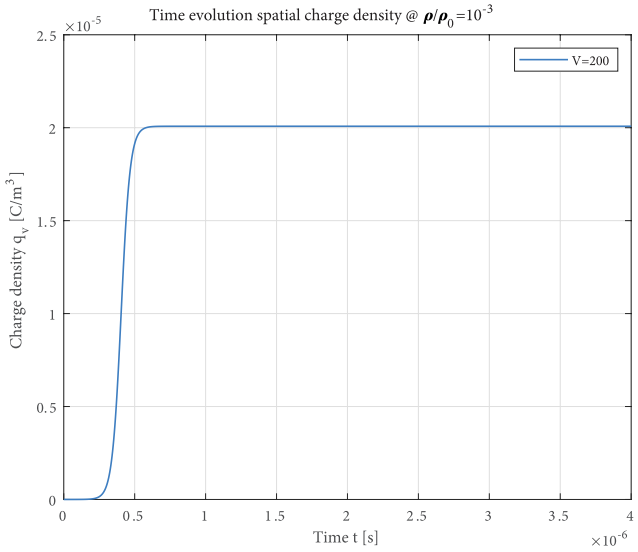

Fig. 5. Time evolution of charge density accumulated during a 4 μs pulse. Asymptotic regimen is reached after ≈ 0.1 μs.

where V is always constant in time. Then, the electric field at the positive electrode remains always greater than zero if the applied voltage is greater than V_{lim} (V limit value):

$$V_{lim} = \frac{q_V^{gen}}{\epsilon_0 \epsilon_r} \frac{d^2}{2} \tag{8}$$

The relationship between the maximum density charge generated by the pulse radiation q_V^{gen} and the absorbed dose in water, in the chamber measuring point, D_p (see APPENDIX B) it is:

$$q_V^{gen} = \frac{D_p \bullet \bar{S}_w^{gas} \bullet \rho}{w_e} \tag{9}$$

where $\bar{S}_W^{gas}$ is the ratio of the average stopping power of the gas in relation to the water, ρ the density of gas within the chamber, w_e is the medium energy required to produce an ion–electron pair in the gas.

Now V_{lim} can be expressed as a function of the dose-*per*-pulse, the gas density and the distance between the electrodes:

$$V_{lim} = \frac{D_p \bullet \overline{S}_w^{gas} \bullet \rho}{2 w_e \epsilon_0 \epsilon_r} d^2 \tag{10}$$

V_{lim} represents the minimum applied voltage for which the field inside the chamber is greater than zero, as a function of dose-*per*-pulse up to D_p. Therefore, any polarization equal or above V_{lim} guarantees there is no recombination at all.

This simplified model is accurate when considering charge collection at atmospheric pressure ($P = 1013.25$ hPa); when the pressure inside the chamber is lowered, charge collection mechanisms cannot be neglected. Therefore, the maximum charge accumulated in the chamber q_{acc} will be less than the total generated charge q_{gen}, consequently the perturbation of the electric field will decrease. In this condition Equation (10) would be a gross, but conservative, estimation of V_{lim}.

Avoiding uncontrolled discharge regimen

Now it is necessary to consider under which condition the chamber does not reach discharge regimen; in fact, for very high values of D_p, V_{lim} might become large enough (for a numerical example see Eq.(8)) to produce electric fields capable of generating uncontrolled discharges of secondary charges. The Paschen empirical curve [26,27,28] describes the minimum voltage which causes discharges in a gas (breakdown tension) as a function of the product between the pressure of the gas and the distance between the electrodes. The idea is to reduce the density of the gas until V_{lim} is below the breakdown value as provided by the Paschen curve (Fig. 3). From Fig. 3 it is possible to extract the breakdown voltage for a chamber filled with Argon and interelectrode distance $d = 1$ *mm*; such breakdown voltage is around 2000 V at atmospheric pressure but larger than 10000 V when pressure is decreased at 1 hPa.

Ion collection dynamics and evaluation of chamber electric field maximum perturbation

The gas pressure decrease, needed for avoiding uncontrolled discharge regimen, causes an increase in ion drift velocity and, consequently, reduces ion collection time. Collection time can now become shorter than T (which is typically in the range 1 to 4 μs for radio-frequency linacs) and then, ion collection dynamic during the pulse must be taken into account.

It is possible to notice that such collection reduces the overall amount of q_v and then, the intensity of $\boldsymbol{E_{ION}}$ as calculated previously in Equation (3).

This depletion effect can be calculated by considering the accumulation process of the positive charges during the pulse. Assuming that the dose deposition is linear over time, it is possible to write its expressions as:

$$\boldsymbol{D(t) = \frac{D_p t}{T},\ being\ 0 \le t \le T} \tag{11}$$

For any time interval dt, there are both charge generation and collection; let dQ^{gen} be the generated and dQ^{coll} the collected charge.

A dynamic model of charge collection is herein presented in order to give a more accurate estimation of the maximum accumulated charge density, taking into account the effect of the positive charge collection.

When the chamber is uniformly irradiated, the volumetric charge generated per unit of time $\dot{q}_V^{gen}$ is uniform within the chamber volume V and is given by:

$$\dot{q}_V^{gen} = \frac{1}{Vol}\frac{dQ^{gen}}{dt} = \frac{\dot{D}(t)\cdot\overline{S}_w^{gas}\cdot\rho}{w_e} = \frac{D_p\cdot\overline{S}_W^{gas}\cdot\rho}{T\cdot w_e} \tag{12}$$

Where $D(t)$ and D_p are to be considered in water.

The volumetric charge collected by the electrodes per unit of time is:

$$\dot{q}_V^{coll} = \frac{1}{Vol}\frac{dQ^{coll}}{dt} = \frac{q_V\cdot dx\cdot S}{V\cdot dt} = \frac{q_V\cdot\nu_D}{d} \tag{13}$$

where ν_D is the drift speed of the positive ions, which can be calculated as:

$$\nu_D = \mu_0\frac{\rho_0}{\rho}E \tag{14}$$

where μ_0 and ρ_0 are respectively the mobility and the density at Normal Temperature and Pressure conditions (NTP), and ρ is the density at chamber working conditions.

The collected volumetric charge density then becomes:

$$\dot{q}_V^{coll} = \frac{q_V\cdot\mu_0\cdot\left(\frac{\rho_0}{\rho}\right)\cdot\boldsymbol{E}}{d} \tag{15}$$

In order to simplify the analytical solution of the differential equation by eliminating the space dependence of q_v, it is useful to assume a homogeneous electrical field inside the chamber. By assigning to the electrical field in each moment the minimum value assumed in the space ($\mathbf{E}(x,t) = \mathbf{E}(0,t)$, at the cathode position) the depletion effect is obviously underestimated. Consequently, the perturbing effect of the accumulated charge is overestimated; therefore, such model provides conservative results on chamber accuracy.

As long as it is:

$$\boldsymbol{E}(\mathbf{0},\mathbf{t}) = \left(\frac{V}{d} - \frac{q_V}{2\varepsilon_0\varepsilon_r}d\right) \tag{16}$$

then Equation (15) becomes:

$$\dot{q}_V^{coll} = \frac{q_V\cdot\mu_0\cdot\left(\frac{\rho_0}{\rho}\right)}{d}\cdot\left(\frac{V}{d} - \frac{q_V}{2\varepsilon_0\varepsilon_r}d\right) \tag{17}$$

By combining the generated and collected charge rates, it is possible to write a differential equation for the net charge rate:

$$\dot{q}_V = \frac{D_p\cdot\overline{S}_W^{gas}\cdot\rho\cdot\left(\frac{\rho}{\rho_0}\right)}{T\cdot w_e} + \frac{\mu_0\cdot\left(\frac{\rho_0}{\rho}\right)}{2\varepsilon_0\varepsilon_r}\cdot q_V^2 - \frac{\mu_0\cdot\left(\frac{\rho_0}{\rho}\right)\cdot V}{d^2}\cdot q_V \tag{18}$$

Equation (18) can be seen as:

$$\dot{q}_V = Aq_V^2 + Bq_V + C \tag{19}$$

where:

$$\begin{cases} A = & \dfrac{\mu_0\cdot\left(\frac{\rho_0}{\rho}\right)}{2\epsilon_0\epsilon_r} \\ B = & -\dfrac{\mu_0\cdot\left(\frac{\rho_0}{\rho}\right)\cdot V}{d^2} \\ C = & \dfrac{D_p\cdot\overline{S}_W^{GAS}\cdot\rho\cdot\left(\frac{\rho}{\rho_0}\right)}{T\cdot w_e} \end{cases} \tag{20}$$

Such differential equation can be solved analytically; the general solution is a monotonous function respect to t, and, therefore, the maximum accumulated charge density q_V^{MAX} is less than its asymptotic value, given by:

$$\lim_{t\to\infty} q_V(t) = -\frac{B + \sqrt{B^2 - 4AC}}{2A} \equiv q_V^{MAX} \tag{21}$$

It is well worth noting that $q_v(t)$ explicitly depends on the instantaneous dose rate per pulse (IDP) that is equal to D_p/T, it is positively monotonous respect to it, and it goes to zero for $D_p/T \to 0$. Such assumption means that when IDP decreases there is no charge accumulation.

The value calculated here is used to estimate the value of E_{ION}^{MAX}, which will be used below to estimate the maximum measurement uncertainty related to the electric field variation, as hereinafter discussed.

The choice of a voltage $V < V_b$ allows to be out of the discharge regimen, but the presence of an appreciable bulk electric charge could cause an error on the measurement of the dose per pulse.

The proper choice of the operating parameters guarantees that the chamber never operates in discharge regimen, even though the possibility of operating in proportional region cannot be excluded. In the following, an estimation of the maximum overall inaccuracy (sensitivity respect to the variation of the electric field/ difference respect to the ionization chamber regimen) is provided.

When an active dosimeter operates in the proportional regimen its response is given by:

$$Q_{coll} = \alpha \bullet Q_{gen} \bullet \boldsymbol{E} \tag{22}$$

Where Q_{coll} is the collected charge, Q_{gen} is the generated charge which is proportional to the absorbed dose per pulse D_p, α is the proportionality coefficient and $\boldsymbol{E} = V/d$ is the electric field.

Then, using Eq.(22), it is possible to calculate the value of Q_{gen} and, thus, the value of the dose per pulse. Equation (22) holds when the electric field has the same value everywhere within the active volume of the chamber.

According to the previous analysis, if a bulk electric charge is present, the electric field inside is no longer uniform. The maximum variation ΔE_{max} occurs at the electrodes and when $t = T$, when bulk electric charge reaches its maximum value, that is $|\Delta E_{max}| \leq |E_{ion}(0,T)|$.

Then, from Eq. (22), it is possible to estimate a relative uncertainty on the collected charge (reading of the chamber) which is:

$$\left|\frac{\Delta Q_{coll}}{Q_{coll}}\right| = \left|\frac{\mathbf{\Delta E}}{\mathbf{E_0}}\right| \leq \frac{|\boldsymbol{E}_{\mathbf{ion}}(0,T)|}{V} d = \frac{q_V^{MAX} \bullet d^2}{2 \bullet \varepsilon_0 \varepsilon_r \bullet V} \tag{23}$$

In such condition, by properly choosing the dosimeter parameters and, in particular, by suitably reducing the gas density ρ, it is possible to dramatically reduce the ion electric field E_{ion}, (being $E_{ion} \propto q_V^{MAX}$) and, thus, the value of the experimental uncertainty until the desired uncertainty is achieved. It should be noticed that the maximum field perturbation is also related to IDP (Eqs. (20)–(21)) and tends to be negligible for small IDP.

A description of the charge and electric field spatial distribution inside the chamber valid in the limit of charge collection time $\tau \ll T$ and negligible electric field perturbation (which represent the ALLS operating conditions), can be found in the Appendix C.

Results

Using the theory described above, it is possible to design a gas chamber for FLASH beam dosimetry.

The ionization chamber has two innovative features:

- Chamber cavity is filled with a noble gas to prevent the capture of ionized electrons and then the production of negative ions;
- the noble gas pressure inside the cavity is adjustable according to the maximum dose per pulse to be measured with any required accuracy respect to electric field perturbation.

The operational flowchart for measuring a beam with a dose per pulse D_p is here summarized step by step:

1. calculate q_V^{gen} (the charge density per unit of volume generated by the pulse inside the chamber) by using Equation (B.3);
2. calculate V_{lim} (the minimum value of the voltage applied to the electrodes necessary to obtain non-zero field, thus avoiding direct recombination);
3. set the chamber polarizationV_{op}, decrease the gas density ρ (and therefore the gas pressure) until $V_{op} > V_{lim}$;
4. consider the Paschen curve and check that chamber does not operate in uncontrolled discharge regimen; if so, further decrease ρ until chamber operates out of such regimen.

These steps guarantee that chamber operates with no recombination and out of discharge regimen, but not necessarily out of proportional regimen; in order to determine the intrinsic accuracy (related to variation of the electric field due to ionized charges), further steps are needed:

5. Set the maximum acceptable value of inaccuracy on the measurement, caused by the perturbation of the electric field over the total range of dose-*per*-pulse to be investigated.
6. Evaluate such inaccuracy by using Eq.(22); if the desired accuracy is not met, decrease again the density ρ until such value is met.

The numerical estimation of the ALLS operating parameters needed to comply with the requests 1–6 is herein detailed, for a 40 Gy dose per pulse and a desired accuracy better than 1 %. The polarization voltage is 200 V and the inter electrode distance d is 1 mm.

A first rough estimate of the maximum allowed pressure is given by Equation (10) and it is 1.42 hPa. We are aware that even though the evaluation through Equation (10) of the first constraint is quite approximate and maybe even at 4 hPa the relation 200 $V > V_{lim}$ is verified, the maximum operative chamber pressure should be in the range [1.42–4] hPa. A more refined model to determinate the maximum pressure is out of the scope of this work since the defined range is already quite strict.

A good estimation of the accumulated charge inside the chamber during a pulse is essential to give a correct value for the maximum electric field perturbation.

The correct estimation of such perturbation requires the adoption of a more accurate model which, still in a conservative mode, takes into account that, at lower pressure, the positive ions collecting is not negligible.

If q_v^{max} is roughly assumed to be the generated charge q_{gen}, such perturbation would be estimated larger than 70 % for P = 1.42 hPa. However, due to the emptying effect, q_v^{max} is significantly smaller than q_{gen}. The dynamic model provides then a more precise estimation of such perturbation, resulting slightly higher than 1 % at 1.42 hPa and around 9 % at 4 hPa.

To further reduce the chamber perturbation, the chamber operating pressure must be reduced at 1 hPa (perturbation around 0.6 %). The operating parameters are summarized in Table 1.

In the chamber working conditions defined above, the spatial dependence of the electric field was also investigated, and a model is presented in Appendix C. Even though such model is not conservative, it is now possible to evaluate and compare the results obtained with the previous analysis, it is still useful to evaluate the consistency of this description with the dynamic model presented in this work. In particular, by using equation (C.9), it is then possible to calculate the maximum electric field perturbation; at $P = 1.42$ hPa, perturbation is around 0.6 %, which is smaller but significantly close to the value obtained by the conservative model (around 1 %).

We also report in Table 2 the uncertainty budget for the parameters involved in the calculation of the chamber maximum electric field perturbation (equation (23)):

Therefore, it is possible to estimate an error of about 4 % when calculating the maximum electric field perturbation.

The theoretical determination of the maximum variation of the electric field identifies the additional uncertainty associated to dose measurements with ALLS chamber due to the large dose per pulse measurements range; the overall uncertainty estimation of the dose measurement is beyond the scope of the current paper and will be determined experimentally after realizing and testing prototypes. Several factors, such as constancy of internal pressure and mechanical integrity will be considered.

Conclusions

The theory and the conceptual design discussed in this manuscript show how to realize a gas chamber capable of measuring dose per pulse values up to 40 Gy delivered in a few microseconds.

The ALLS chamber has been patented [23] and the first prototypes are currently under test (see Fig. 4) [35]. There are two main engineering challenges to deal with:

- chamber body must hold a pressure gauge up to 1013 hPa;
- chamber must be precisely sealed, and the gas pressure must be set according to the dose per pulse value to be measured.

These engineering issues and the experimental results will be presented and discussed in the future.

Even with all the simplifications introduced, the theory shows that above a given value of D_p, pulse duration significantly impacts chamber behaviour. Therefore, the dose per pulse is no longer the only parameter to be considered, as in the case of estimation of k_{sat} with IORT linacs [24].

The behaviour of the ALLS chamber, where the recombination effect can be neglected, is only influenced in the UHDP context by the residual perturbative effects of the field generated by the maximum accumulated charge in the chamber. This effect, as shown by the C parameter in Eq. (20), depends on the charge production rate which is linked to the instantaneous dose rate during the pulse D_p/T. Once this quantity has been fixed, the chamber response is practically independent from pulse duration. The only exception is the case where T value is comparable with the charges collection time: in this condition the solution does not reach the asymptotic value and the electric field perturbation is reduced (see Fig. 5, where asympotic value is reached after around 0.15 μs).

Therefore, the peculiar chamber architecture should make it suitable for dose measurement within a water and water equivalent phantom.

The authors expect that the theory and the design of ALLS chamber here presented could help to solve the challenge of a precise dosimetric characterization of UHD and UHDR beams, which is still essential for the FLASH effect full comprehension and use.

Declaration of Competing Interest

F. Galante, G. Mariani, M. Pacitti and G. Felici are SIT employees; G. Felici is a SIT shareholder; A. Gasparini received a grant for a post doc position funded by SIT S.p.A. The remaining authors declare that they have no known competing financial interests or personal relationships that could have appeared to influence the work reported in this paper.

Acknowledgments

The authors deeply thank Prof. S. Faetti for discussing and revising the manuscript and Mrs. Ilaria Breglia for the English revision.

Appendix A. Evaluation of ion charge collection time

An estimate of the charge collection time evolution between two beam pulses can be obtained focusing on positive ions only due to their lower mobility with respect to the electrons. In a first order approximation, the effect of E_{ION} on the positive ions collection can be neglected and, in this assumption, an approximate result can be obtained focusing on the positive ion farthest from the cathode.

Therefore, the drift speed is only influenced by the polarization field $\boldsymbol{E_0}$:

$$v_d = \mu E_0 = \mu \frac{V}{d} \tag{A.1}$$

where μ is the ions mobility, V is chamber polarization potential and d is the distance between the chamber walls. It is straightforward to obtain the ion collection time:

$$T_{cc} = \frac{d}{v_d} = \frac{d^2}{\mu V} \tag{A.2}$$

As an example, the collection time of the positive ions in air ($\mu = 1.6\mathrm{T}cm^2\,s^{-1}\,\mathrm{V}^{-1}$) for the Advanced Markus chamber ($V = 300$ V, $d = 1$ mm) is approximately $T_{cc} \sim 20$ μs. Supposing that the beam pulse frequency is $f = 250$ Hz it is verified that the charge collection time T_{cc} is orders of magnitude smaller than the interval between two pulses $\Delta t = 1/f = 4$ ms; hence the collection mechanisms can be preliminarily studied for a single pulse without loss of generality.

The assumption holds true even with the more refined charge collection description developed in this work if the pressure of the Argon in the cavity is taken as a parameter that can be changed freely. In order to provide a numerical conservative estimation of the positive ions collection time, the following assumptions are made:

1. The collection time is calculated for a positive ion in proximity of the anode (i.e. the path ions have to cross is d);
2. the electric field value inside the chamber $\boldsymbol{E}$ is assumed to be its minimum value (at anode position, $x = 0$, and $t = T$, when E_{ION} is maximum) as calculated by using Eq.3–7**:**

$$\mathbf{E}(x=0,\, t=T) = \boldsymbol{E_{ION}}(x=0,\, t=T) + \boldsymbol{E}_0 = -\frac{q_V^{gen}}{\epsilon_0 \epsilon_r}\frac{d}{2} + \frac{V}{d} \tag{A.3}$$

3. the ration of the mass stopping powers between Argon and water $\overline{S}_w^{Ar}$ assumed to be 1 (such value is less than 1 up to 15 MeV [30]).

The value of the generated volumetric charge q_V^{gen} can be calculated by using Equation (9). Given a an interelectrode distance $d = 1$ mm, filled with Argon at a pressure of 1 Atm ($\rho_0 = 1.66$ kg/m^3), exposed to a dose per pulse $D_p = 40$ *Gy*, the generated volumetric charge during the pulse is $q_V^{gen} \approx 2.55\mathrm{C/m}^3$. The limit voltage is then readily obtained from Equation:

$$V_{lim} = \frac{q_V^{gen}}{\epsilon_0 \epsilon_r}\frac{d^2}{2} \approx 1.44{\cdot}10^5\ \mathrm{V} \tag{A.4}$$

This value is higher than the polarization voltage chosen for the ALLS chamber ($V = 200$ V); in order to reduce V_{lim} the generated charge q_V must be reduced. Since the density of the gas is proportional to its pressure (i.e. $\rho \propto p$) and the generated volumetric charge is proportional to the density of the gas in the chamber ($q_V \propto \rho$, Equation (9)), it is possible to reduce the voltage limit by decreasing the pressure of the gas in the chamber. As an example, by reducing the pressure to 1 hPa a polarization voltage of 200 V is enough to avoid recombination as explained in the Theory Section.

The pressure reduction has also the effect of increasing the mobility of the positive ions as follows:

$$\mu = \mu_0 \frac{\rho_0}{\rho} \tag{A.5}$$

Putting all the equations together, the formula for the estimate of positive ion collection time is:

$$T_{cc} = \frac{d}{v_d} = \frac{d}{\mu E} \approx \frac{d}{\mu_0 \frac{\rho_0}{\rho}\left(\frac{V}{d} - \frac{q_V}{\epsilon_0 \epsilon_r}\frac{d}{2}\right)} = \frac{d}{\mu_0 \frac{\rho_0}{\rho}\left(\frac{V}{d} - \frac{D_p \rho}{\epsilon_0 \epsilon_r(w_e)}\frac{d}{2}\right)} \approx 0.1\,\mu s \tag{A.6}$$

In conclusion a reduction of the chamber gas leads to a charge collection time order of magnitude smaller than the pulses time interval even for high dose per pulse, at least for radiofrequency powered linacs, where maximum Pulse Repetition Frequency is less than 1000 Hz [34].

Appendix B. Generated charged inside an ionization chamber relative to dose in water

Considering an ionization chamber filled with a mass of gas m_{gas} with density ρ_0 at NTP, when the gas in the cavity absorbs a medium dose D_{gas} the generated charge inside the chamber is:

$$q^{gen} = \frac{D_{gas} \bullet m_{gas}}{w_e^{gas}} \tag{B.1}$$

where w_e^{gas} is the medium energy required to produce an electron–ion pair in the gas. The relationship between the dose to the gas and the dose to water D_w is given by the Bragg-Gray cavity theory [31,32,33]:

$$D_w = D_{gas} \overline{S}_{gas}^{w} \tag{B.2}$$

where $\overline{S}_{gas}^{w}$ is the ratio between the mass stopping power of water and gas, assuming that perturbative factors due to the wall chambers are negligible.

Putting together Equations (B.1) and (B.2) the result is the expression for the volumetric generated charge inside a chamber with a cavity of volume V in relation to the Dose to water:

$$q_V^{gen} = \frac{q^{gen}}{\mathcal{V}} = \frac{D_w \overline{S}_w^{gas} \rho}{w_e} \tag{B.3}$$

Appendix C. Spatial dependence of the accumulated volumetric charge

The electric field and the charge distribution between ALLS ionization chamber plates can be described by the following set of partial differential equation [29]:

$$\frac{\partial \rho_+(x,t)}{\partial t} = \dot{Q}(x,t) - \frac{\partial}{\partial x}[E(x,t)\mu_+ \rho_+(x,t)] \tag{C.1}$$

$$\frac{\partial \rho_e(x,t)}{\partial t} = \dot{Q}(x,t) - \frac{\partial}{\partial x}[E(x,t)\mu_e \rho_e(x,t)] \tag{C.2}$$

$$\frac{\partial E(x,t)}{\partial x} = \frac{1}{\varepsilon}[\rho_+(x,t) - \rho_e(x,t)] \tag{C.3}$$

Where:

- $\boldsymbol{\rho}_+(\boldsymbol{x},\boldsymbol{t})$ and $\boldsymbol{\rho_e}(\boldsymbol{x},\boldsymbol{t})$ are the volumetric charge densities of positive ions and electrons, respectively.
- $\dot{\boldsymbol{Q}}(\boldsymbol{x},\boldsymbol{t})$ is the charge generation rate produced by the irradiation.
- ε is the dielectric constant of Argon.
- $\boldsymbol{E}(\boldsymbol{x},\boldsymbol{t})$ is the electric field.

It is assumed that the dose deposition is linear over time and uniform over space. Then, dropping the spatial dependence over the charge generation rate and expressing its time dependence in function of the dose per pulse $\boldsymbol{D_p}$ and the pulse duration $\boldsymbol{T}$:

$$\dot{Q} = \frac{d}{dt}[Q(t)] = \frac{d}{dt}\left[\frac{D_p \cdot \overline{S}_W^{gas} \cdot \varrho}{T \cdot w_e} t\right] = \frac{D_p \cdot \overline{S}_W^{gas} \cdot \rho}{T \cdot w_e} \tag{C.4}$$

where $\overline{S}_W^{gas}$ is the ratio of the average stopping power of the gas in relation to the water, ρ the density of gas within the chamber, w_e is the medium energy required to produce an ion–electron pair in the gas.

At the ALLS chamber (1 hPa) operating pressure, the following assumptions can be made:

- the characteristic time τ describing the transient dynamic of charge accumulation is shorter than the pulse duration T. Therefore, for most of the pulse duration, the system is characterized by time stationary solution $\frac{\partial \rho_+(x,t)}{\partial t} = 0$;
- charge accumulation is greatly reduced, thus the perturbating electric field is smaller than the polarization electric field $\boldsymbol{E}_0 = V/\boldsymbol{d}$; therefore the total field can be written as:

$$\frac{\Delta E}{E} \approx 0 \rightarrow \boldsymbol{E}(x) \approx \boldsymbol{E}_0 = \frac{V}{\boldsymbol{d}} \tag{C.5}$$

The equation (C.1) can be solved in the steady state condition ($\frac{\partial \rho_+(x,t)}{\partial t} = 0$):

$$\dot{Q} = E_0 \mu_+ \frac{\partial}{\partial x}[\rho_+(x, t \gg \tau)] \tag{C.6}$$

The solution is:

$$\rho_+(x, t \gg \tau) = \frac{\dot{Q} d^2}{E_0 \mu_+} - \frac{\dot{Q} d}{E_0 \mu_+} x = \frac{\dot{Q} d}{V \mu_+}(d - x) \tag{C.7}$$

Considering that the mobility of the electrons is order of magnitude greater than positive ions, their contribution to the total (net) charge accumulated inside the chamber is negligible. Therefore, it is possible to derive an expression for $\boldsymbol{E}$ considering only the positive charge contribution.

The equation of the electric field due to the positive ions can be obtained from equation (C.3):

$$\boldsymbol{E_{ION}}(x, t \gg \tau) = \frac{\dot{Q}}{\varepsilon V \mu_+} d \left[-\frac{x^2}{2} + dx - \frac{d^2}{4} \right] \tag{C.8}$$

The estimated uncertainty of the chamber is evaluated with the following relation:

$$\left| \frac{\mathbf{\Delta E}}{\mathbf{E_0}} \right| \leq \frac{|\mathbf{E_{ION}}(\mathbf{0}, \mathbf{t} \gg \boldsymbol{\tau})|}{V} d = \frac{\dot{Q}}{4 \varepsilon V^2 \mu_+} d^4 \tag{C.9}$$

Plots for the positive ion's density and the perturbative electric field in the chamber are presented in Figs. C.1-C.2.

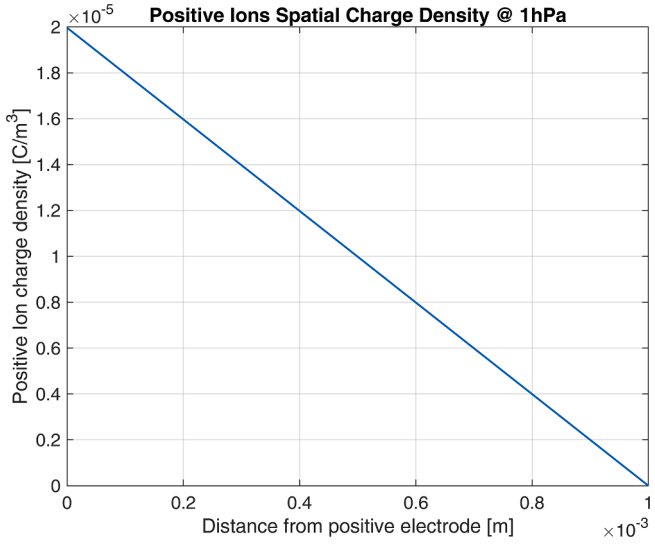

Fig. C1. Positive Ions charge density.

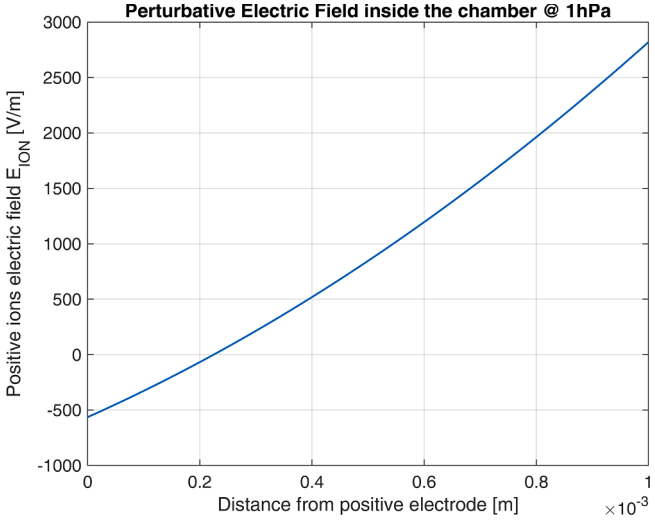

Fig. C2. Perturbative Electric Field inside the chamber.

References

[1] Favaudon V, Caplier L, et al. Ultrahigh dose-rate FLASH irradiation increases the differential response between normal and tumor tissue in mice. Sci Transl Med 2014. https://doi.org/10.1126/scitranslmed.3008973. 6:245ra93-245ra93.

[2] Montay-Gruel P, Acharya MM, et al. Long-term neurocognitive benefits of FLASH radiotherapy driven by reduced reactive oxygen species. PNAS 2019;116: 10943–51. https://doi.org/10.1073/pnas.1901777116.

[3] Vozenin M-C, Fornel PD, et al. The Advantage of FLASH Radiotherapy Confirmed in Mini-pig and Cat-cancer Patients. Clin Cancer Res 2019;25:35–42. https://doi.org/10.1158/1078-0432.CCR-17-3375.

[4] Bourhis J, Montay-Gruel P, et al. Clinical translation of FLASH radiotherapy: Why and how? Radiother Oncol 2019;139:11–7. https://doi.org/10.1016/j.radonc.2019.04.008.

[5] Spitz DR, Buettner GR, Petronek MS, St-Aubin JJ, et al. An integrated physico-chemical approach for explaining the differential impact of FLASH versus conventional dose rate irradiation on cancer and normal tissue responses. Radiother Oncol 2019;139:23–7. https://doi.org/10.1016/j.radonc.2019.03.028.

[6] FLASH radiotherapy: from preclinical promise to the first human treatment. Physics World 2019. https://physicsworld.com/a/flash-radiotherapy-from-preclinical-promise-to-the-first-human-treatment/ [accessed July 21, 2021].

[7] Durante M, Bräuer-Krisch E, Hill M. Faster and safer? FLASH ultra-high dose rate in radiotherapy. Br J Radiol 2018;91:20170628. https://doi.org/10.1259/bjr.20170628.

[8] Bourhis J, Sozzi WJ, et al. Treatment of a first patient with FLASH-radiotherapy. Radiother Oncol 2019;139:18–22. https://doi.org/10.1016/j.radonc.2019.06.019.

[9] Jorge PG, Jaccard M, et al. Dosimetric and preparation procedures for irradiating biological models with pulsed electron beam at ultra-high dose-rate. Radiother Oncol 2019;139:34–9. https://doi.org/10.1016/j.radonc.2019.05.004.

[10] McManus M, Romano F, et al. The challenge of ionisation chamber dosimetry in ultra-short pulsed high dose-rate Very High Energy Electron beams. Sci Rep 2020; 10:9089. https://doi.org/10.1038/s41598-020-65819-y.

[11] Subiel A, Moskvin V, et al. Challenges of dosimetry of ultra-short pulsed very high energy electron beams. Physica Med 2017;42:327–31. https://doi.org/10.1016/j.ejmp.2017.04.029.

[12] Bazalova-Carter M, Esplen N. On the capabilities of conventional x-ray tubes to deliver ultra-high (FLASH) dose rates. Med Phys 2019;46:5690–5. https://doi.org/10.1002/mp.13858.

[13] Schüller A, Heinrich S, et al. The European Joint Research Project UHDpulse – Metrology for advanced radiotherapy using particle beams with ultra-high pulse dose rates. Physica Med 2020;80:134–50. https://doi.org/10.1016/j.ejmp.2020.09.020.

[14] Gómez F, et al. Development of an ultra-thin parallel plate ionization chamber for dosimetry in FLASH radiotherapy. Med Phys 2022:1–10. https://doi.org/10.1002/mp.15668.

[15] Marinelli M, Felici G., et al. Design, realization, and characterization of a novel diamond detector prototype for FLASH radiotherapy dosimetry. Med Phys, 10.1002/mp.15473.

[16] Marinelli M, et al. Design, realization, and characterization of a novel diamond detector prototype for FLASH radiotherapy dosimetry. MEd Phys 2022;2022. https://doi.org/10.1002/mp.15473.

[17] Esplen N, Mendonca MS, Bazalova-Carter M. Physics and biology of ultrahigh dose-rate (FLASH) radiotherapy: a topical review. Phys Med Biol 2020. https://doi.org/10.1088/1361-6560/abaa28. 65:23TR03.

[18] Fouillade C, Favaudon V, et al. Les promesses du haut débit de dose en radiothérapie. Bull Cancer 2017;104. https://doi.org/10.1016/j.bulcan.2017.01.012.

[19] Di Martino F, Barca P, et al. FLASH Radiotherapy With Electrons: Issues Related to the Production, Monitoring, and Dosimetric Characterization of the Beam. Front Phys 2020. https://doi.org/10.3389/fphy.2020.570697.

[20] Montay-Gruel P, Petersson K, et al. Irradiation in a flash: Unique sparing of memory in mice after whole brain irradiation with dose rates above 100 Gy/s. Radiother Oncol 2017;124:365–9. https://doi.org/10.1016/j.radonc.2017.05.003.

[21] Schüller E, Acharya M., et al. Ultra-high dose rate electron beams and the FLASH effect: From preclinical evidence to a new radiotherapy paradigm. Med Phys 2022: mp.15442. 10.1002/mp.15442.

[22] Andreo P., Burns D., et al. Absorbed Dose Determination in External Beam Radiotherapy. An International Code of Practice for Dosimetry based on Standards of Absorbed Dose to Water.

[23] Di Martino F. et al. Metodo per il controllo del trattamento radioterapico di malati oncologici e dispositivo di controllo, Italian Patent Request. 102021000019520. pdf.

[24] Di Martino F, Giannelli M, Traino AC, Lazzeri M. Ion recombination correction for very high dose-per-pulse high-energy electron beams. Med Phys 2005;32:2204–10. https://doi.org/10.1118/1.1940167.

[25] Boag JW, Hochhäuser E, Balk OA. The effect of free-electron collection on the recombination correction to ionization measurements of pulsed radiation. Phys Med Biol 1996;41:885–97. https://doi.org/10.1088/0031-9155/41/5/005.

[26] Lieberman MA, Lichtenberg AJ. Principles of Plasma Discharges and Materials Processing. John Wiley & Sons; 2005.

[27] Paschen F. Ueber die zum Funkenübergang in Luft, Wasserstoff und Kohlensäure bei verschiedenen Drucken erforderliche Potentialdifferenz. Ann Phys 1889;273: 69–96. https://doi.org/10.1002/andp.18892730505.

[28] Macheret SO, Shneider MN. Kinetic modeling of the Townsend breakdown in argon. Phys Plasmas 2013;20:101608. https://doi.org/10.1063/1.4823471.

[29] Gotz M, Karsch L, Pawelke J. A new model for volume recombination in plane-parallel chambers in pulsed fields of high dose-per-pulse. Phys Med Biol 2017;62: 8634–54. https://doi.org/10.1088/1361-6560/aa8985.

[30] https://physics.nist.gov/PhysRefData/Star/Text/ESTAR.html n.d.

[31] Ma C, Nahum AE. Bragg-Gray theory and ion chamber dosimetry for photon beams. Phys Med Biol 1991;36:413–28. https://doi.org/10.1088/0031-9155/36/4/001.

[32] Khan FM. The physics of radiation therapy. 3rd ed. Philadelphia: Lippincott Williams & Wilkins; 2003.

[33] Attix. Introduction to Radiological physics and radiation dosimetry.pdf.WILEY-VCH Verlag GmbH & Co. KGaA (2004).

[34] Jolly S., Owen H., et al. Technical challenges for FLASH proton therapy. Phys Med, 10.1016/j.ejmp.2020.08.005.

[35] Soliman Y.S., Pellicioli P., et al. A comparative dosimetry study of an alanine dosimeter with a PTW PinPoint chamber at ultra-high dose rates of synchrotron radiation. Phys Med, 10.1016/j.ejmp.2020.03.007.